RNA Folding and Misfolding of the Hammerhead Ribozyme

Gurminder S. Bassi, Niels Erik Møllegaard,‡ Alastair I. H. Murchie, and David M. J. Lilley*

CRC Nucleic Acid Structure Research Group, Department of Biochemistry, The University of Dundee, Dundee DD1 4HN, U.K.

Received December 18, 1998; Revised Manuscript Received January 11, 1999

ABSTRACT: The hammerhead ribozyme undergoes a well-defined two-stage folding process induced by the sequential binding of two magnesium ions. These probably correspond to the formation of domain 2 (0−500 μM magnesium ions) and domain 1 (1−20 mM magnesium ions), respectively. In this study we have used fluorescence resonance energy transfer (FRET) to analyze the ion-induced folding of a number of variants of the hammerhead ribozyme. We find that both A14G and G8U mutations are highly destabilizing, such that these species are essentially unfolded under all conditions. Thus they appear to be blocked in the first stage of the folding process, and using uranyl-induced photocleavage we show that the core is completely accessible to this probe under these conditions. Changes at G5 do not affect the first transition but appear to provide a blockage at the second stage of folding; this is true of changes in the sugar (removal of the 2′-hydroxyl group) and base (G5C mutation, previously studied by comparative gel electrophoresis). Arrest of folding at this intermediate stage leads to a pattern of uranyl-induced photocleavage that is changed from the wild-type, but suggests a structure less open than the A14G mutant. Specific photocleavage at G5 is found only in the wild-type sequence, suggesting that this ion-binding site is formed late in the folding process. In addition to folding that is blocked at selected stages, we have also observed misfolding. Thus the A13G mutation appears to result in the ion-induced formation of a novel tertiary structure.

RNA molecules must undergo precise folding into the correct three-dimensional structure to be biologically active. The highly charged polyelectrolyte backbone results in an important electrostatic component in the process, and metal ions play a critical role in stabilizing the folded structures. The hammerhead ribozyme (*1*−*4*) provides a particularly useful system for the study of ion-induced RNA folding. First, it is a relatively small RNA species that undergoes a well-defined two-stage folding process in response to the addition of magnesium ions (*5, 6*). Second, the folding can be correlated with functional activity (*7*), i.e., the rate of ribozyme cleavage. Last, there are a number of crystal structures of the hammerhead ribozyme available (*8*−*11*) that provide considerable insight into the interpretation of the folding process.

The hammerhead ribozyme consists of three double-helical stems (e.g., see Figure 1) linked together by the formally single-stranded core of the junction. In the structures of the hammerhead ribozyme observed in the crystal (*8, 9*) there is an approximately coaxial alignment between stems II and III, mediated by the formation of two G·A pairs that form domain 2 of the structure. The 5′ CUGA sequence of the long single-stranded section between stems I and II forms a turn, called domain 1 or the uridine turn, and is believed to be the catalytic core of the ribozyme. In the crystal structures there is a small angle subtended between the axes of helices I and II. Using comparative gel electrophoresis and fluorescence resonance energy transfer (FRET) we have shown that the hammerhead ribozyme is extended in the absence of added divalent metal ions, with a large angle between stems I and II while stem III is approximately perpendicular (*5, 6*). This structure is also consistent with analysis by transient electric birefringence (*12*). Folding into a global structure consistent with that seen in the crystal occurs in two distinct stages. The first stage is induced by the binding of a

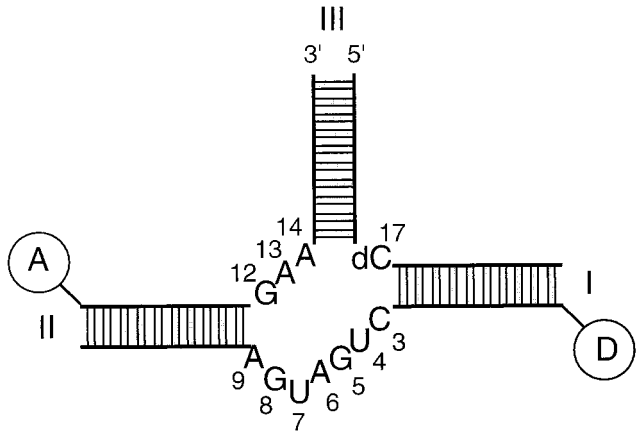

FIGURE 1: Hammerhead constructs used for analysis by FRET. The molecules comprise three strands hybridized together to create the core of the hammerhead with arms each of 10 bp in length. Two of the strands carry a donor (D) and acceptor (A) fluorophore at the 5′ terminus, respectively, while the third is unlabeled. The example shown is vector I−II in which arm I carries the donor (fluorescein) and arm II carries the acceptor (Cy3). In the spectroscopic experiments C17 is replaced by deoxyribocytosine to prevent ribozyme cleavage occurring in the presence of magnesium ions.

‡ The Panum Institute, Department of Medical Biochemistry and Genetics, Biochemistry B, Panum Instituttet, Københavns Universitet, Blegdamsvej 3c, 2200 København N, Denmark.

* To whom correspondence should be addressed. Tel: 44-1382 344243. FAX: 44-1382 201063. E-mail: dmjlilley@bad.dundee.ac.uk.

10.1021/bi982985r CCC: $18.00
Published on Web 02/23/1999

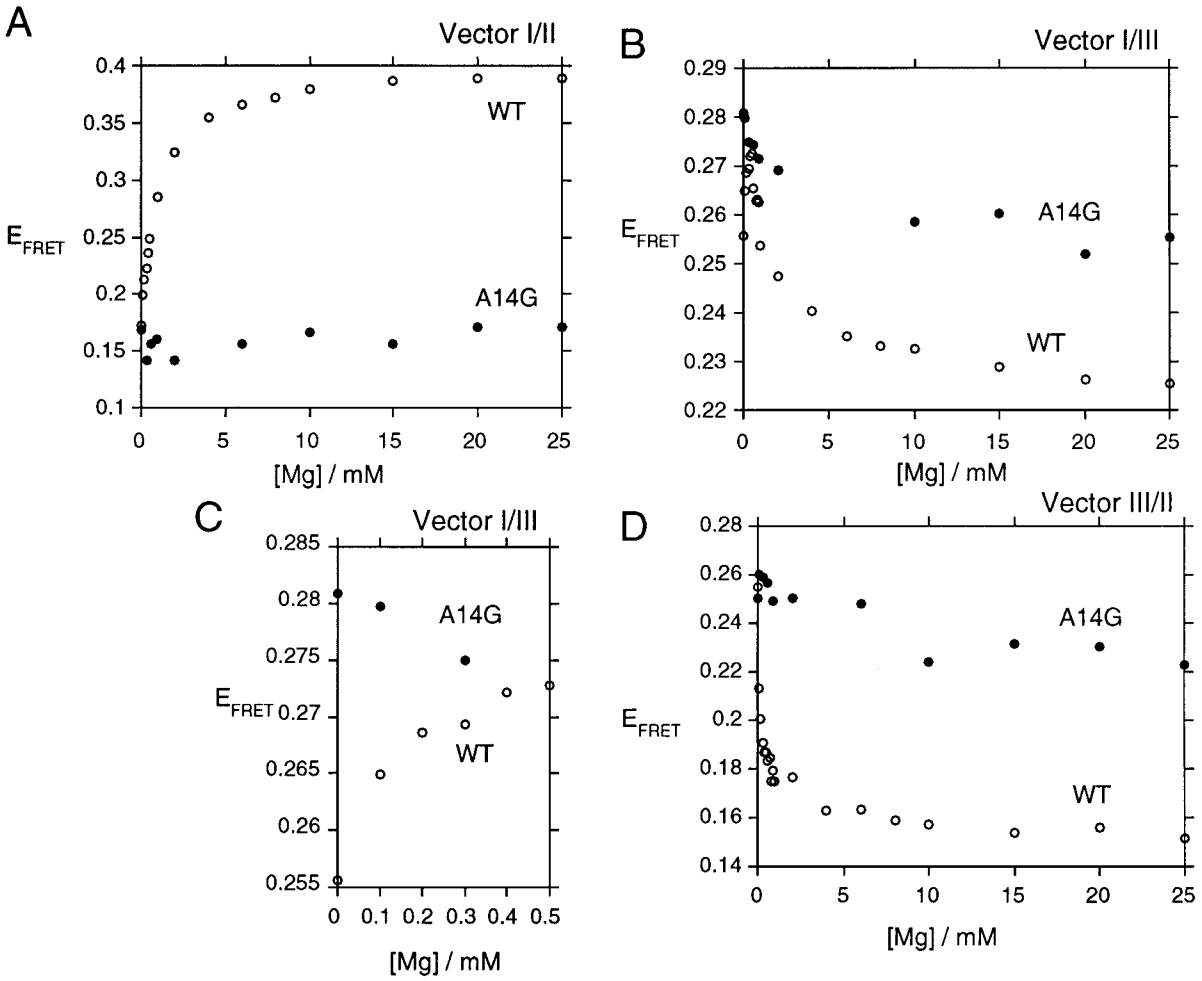

FIGURE 2: Comparison of the ion-induced folding of wild-type and A14G mutant hammerhead ribozymes. The calculated efficiency of FRET (E_{FRET}) has been measured for the three end-to-end vectors of the two RNA species as a function of magnesium ion concentration. (A) Plot of E_{FRET} as a function of magnesium ion concentration for vector I−II (labeled with fluorescein at the terminus of arm I and Cy3 at the terminus of arm II). (B) Plot of E_{FRET} as a function of magnesium ion concentration for vector I−III (labeled with fluorescein at the terminus of arm I and Cy3 at the terminus of arm III) over the complete titration range from 0 to 25 mM magnesium ions. (C) Expanded plot of E_{FRET} as a function of magnesium ion concentration for vector I−III, over the titration range from 0 to 500 μM magnesium ions. (D) Plot of E_{FRET} as a function of magnesium ion concentration for vector III−II (labeled with fluorescein at the terminus of arm III and Cy3 at the terminus of arm II). Symbols used in all graphs: ○ wild-type hammerhead sequence, ● A14G mutant sequence.

magnesium ion with an apparent association constant of approximately 10 000 M^{-1}, in the range 0−500 μM magnesium ions. It probably corresponds to the formation of domain 2, but at this stage domain 1 is likely to be unfolded, and stem I is oriented into the same quadrant as stem III. The second stage of the folding process occurs in the range 1−20 mM magnesium ions, and corresponds to the binding of a magnesium ion with an apparent association constant of close to 1000 M^{-1}. The global structure of this final state is in good agreement with that observed in the crystal, and the transition very probably corresponds to the formation of domain 1. A structural transition in the 1−10 mM magnesium ion range has also been detected by observing the fluorescence of 2-aminopurine located at the ribozyme-proximal end of stem I (*13*). Both the intermediate and final states have been characterized by comparative gel electrophoresis (*5*) and FRET (*6*).

The formation of the final structure can be correlated with the acquisition of catalytic activity of the ribozyme. Thus between the intermediate state (500 μM magnesium ions) and the final state (15 mM magnesium ions) the activity rises from virtually zero to a maximum (*7*). It is highly probable that an important part of the mode of action of the ribozyme is a local distortion to achieve the correct juxtaposition of attacking nucleophile and leaving group in the transition state of the reaction. Thus the final folded structure may contain stereochemical stress that can facilitate the trajectory into the transition state, and a form that appears to be close to this has recently been observed in the crystal (*11*).

In the present study we have analyzed the effect of core sequence changes on the folding of the hammerhead ribozyme. We have used FRET to analyze the folding of five variants of the hammerhead ribozyme, with changes targeted to bases expected to participate at different stages of the folding process. We find a number of mutants that appear to be blocked at specific stages of the folding pathway, as well as one that adopts an alternative structure not seen with the wild-type sequence.

RESULTS

Analysis of Folding in the Hammerhead Ribozyme Using Fluorescence Resonance Energy Transfer. We have used FRET to follow the ion-induced folding of the hammerhead ribozyme and sequence variants. In this method we regard

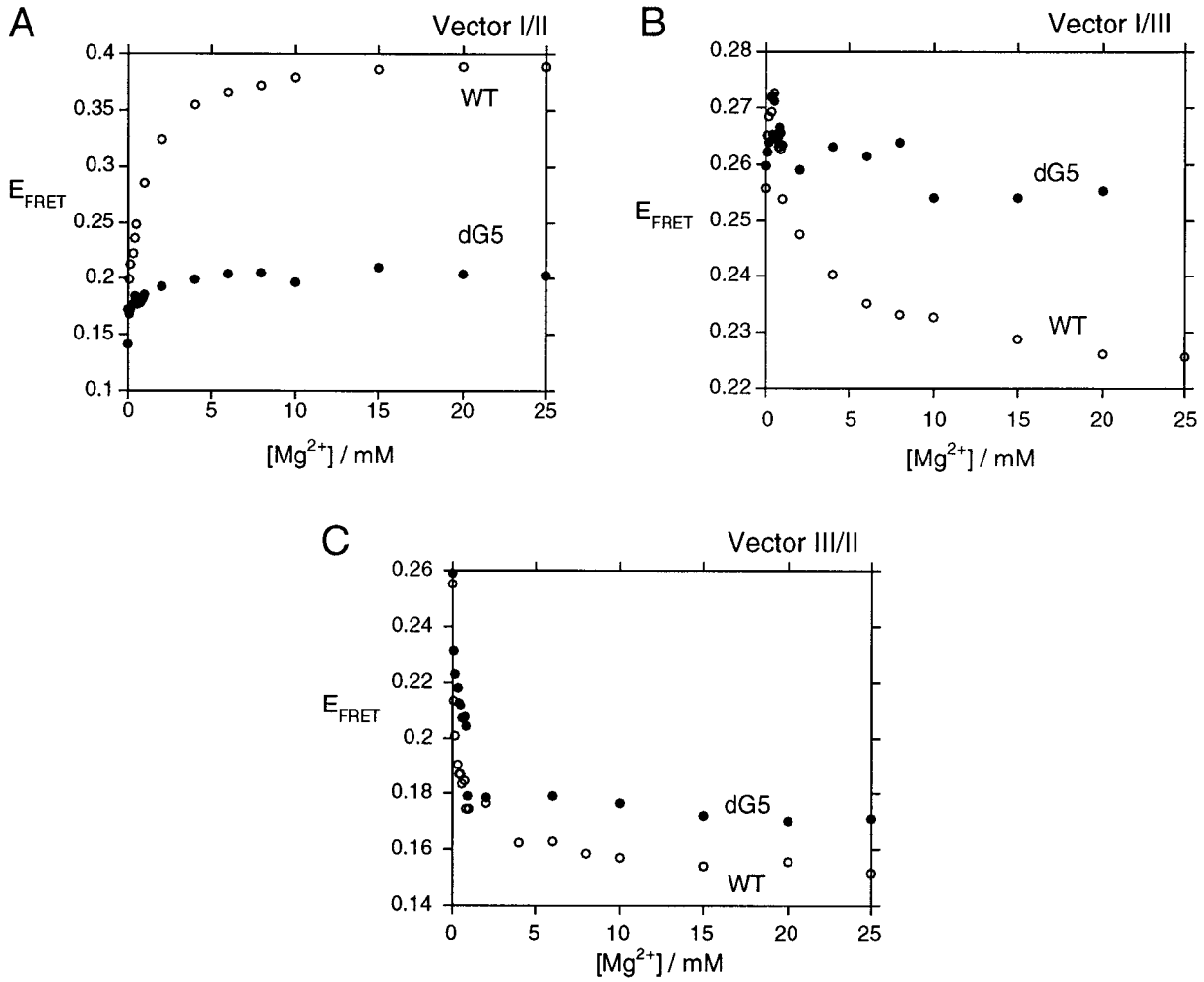

FIGURE 3: Comparison of the ion-induced folding of wild-type and deoxy-G5-modified hammerhead ribozymes. All titrations were carried out over the range from 0 to 25 mM magnesium ions. Plot of E_{FRET} as a function of magnesium ion concentration for vector I−II (A), vector I−III (B) and vector III−II (C). Symbols used in all graphs: ○ wild-type hammerhead sequence, ● deoxy-G5 hammerhead species.

the hammerhead ribozyme as a kind of three-way helical junction and study the variation in the lengths of vectors between fluorophores attached to the termini of different pairs of helices (*6*). If the helices have the same length, the relative lengths will reflect the angles subtended between the different helices. Energy transfer results from a dipolar coupling between the transition moments of the two fluorophores, and the efficiency (E_{FRET}) is therefore inversely dependent on the sixth power of the distance between them. Thus E_{FRET} increases markedly as the distance between the fluorophores becomes shorter. For these experiments, we have constructed a series of hammerhead-related species comprising the core (with deoxyribose substitution at C17 to prevent self-cleavage) and three arms each of 10 bp in length (Figure 1). Fluorescein (donor) and Cy3 (acceptor) fluorophores have been attached to the 5′ ends of arms in a pairwise manner. Cy3 is relatively constrained when attached to the RNA duplex, with an anisotropy (r) of 0.27 in the presence of 90 mM Tris·borate (pH 8.3), 25 mM NaCl. However, the fluorescein is relatively mobile ($r = 0.10$ in the presence of 90 mM Tris·borate (pH 8.3), 25 mM NaCl), and thus dye orientation should not complicate the straightforward interpretation of the FRET results. Each helix in the molecules terminates in a 5′CC sequence to ensure a constant environment for the fluorophores; we have previously found that this provides a well-behaved environment for FRET measurements in nucleic acids (*6*, *14*−*17*). We have calculated efficiencies of FRET using the acceptor normalization method (*18*).

As we have shown in an earlier study (*6*), the variation of FRET efficiency for the three end-to-end vectors of the hammerhead ribozyme as a function of magnesium ion concentration is in good agreement with the previously proposed scheme for ion-induced folding (refer ahead to Figure 8). This is shown by the titration of the three vectors for the natural sequence ribozyme shown in Figure 2 (open symbols). Vector I−II shortens over the entire range of magnesium concentration, eventually achieving an E_{FRET} of 0.38, corresponding to the shortest end-to-end distance in the fully folded structure. Vector I−III exhibits a biphasic behavior, with an initial increase in E_{FRET} over the 0−500 μM range of magnesium ions, followed by a reduction to 0.23 as the concentration is increased to 20 mM. Vector III−II has a special character, as this represents the formation of the coaxial stack between the two helices. In the natural sequence the efficiency falls rapidly over the 0−500 μM range of magnesium ions, as the helix−helix association forms, with a more gentle reduction thereafter as the structure reorganizes to some extent. This property is thus diagnostic for the formation of the II−III helix coaxial association. The global structure of the form occurring in the presence of the higher magnesium ion concentrations is in good agreement

with that found in the crystal (*8, 9*) and in other solution studies (*19, 20*).

A14G Mutation: A Total Folding Block. The mutation A14G changes one of the adenine bases in the oligopurine sequence that comprises the formally single-stranded section between helices II and III; this mutation leaves the hammerhead ribozyme essentially inactive (*7*). A14 participates in the formation of domain 2, which generates the coaxial alignment of helices II and III. Using comparative gel electrophoresis we have previously concluded that this mutation leaves the hammerhead unable to undergo folding from the extended structure that exists in the absence of added metal ions (*21*). We constructed the required fluorescein−Cy3-labeled species and performed a FRET analysis of the magnesium ion induced folding. The results confirm our conclusions from the comparative gel electrophoresis. The results for the A14G mutant (closed symbols) are compared with those of the natural sequence (open symbols) in Figure 2. Vector I−II (Figure 2A) shows almost no change in E_{FRET} over the entire range of magnesium ion concentration, while in the natural ribozyme this exhibits the largest increase. Vector I−III (Figure 2B, C) does not show the initial rise in E_{FRET}, and its eventual reduction is much more modest than that of the wild-type sequence. Last, vector III−II (Figure 2D) exhibits only a very gentle reduction in E_{FRET} with magnesium ion concentration and does not display the pronounced fall in the 0−500 μM magnesium ion concentration range indicative of the formation of the II−III helical stack. The final values of E_{FRET} for the three vectors in the presence of 20 mM magnesium ions (summarized in Figure 8) are little altered from those of the natural sequence ribozyme in the absence of magnesium ions. Thus the FRET experiments support the absence of folding in the A14G hammerhead mutant.

DeoxyG5: A Second Stage Folding Block. G5 lies in the CUGA sequence that ultimately forms the uridine turn (domain 1) of the hammerhead ribozyme. Comparative gel electrophoresis indicated that removal of the 2′-hydroxyl (deoxy-G5), or substitution of the base by cytosine (G5C), allows magnesium ion induced folding to proceed to the first stage, but that further folding was blocked at that point (*21*). The results of FRET analysis of folding (closed symbols) are compared with those of the natural sequence (open symbols) in Figure 3. It is apparent that the folding of the hammerhead ribozyme is severely affected by the removal of the 2′-hydroxyl group at G5. Vector I−II (Figure 3A) shows a small increase in E_{FRET}, rising to 0.20 in magnesium ion concentrations greater than 5 mM. This is considerably lower than the value for the same vector in the natural sequence, showing that the close approach of the ends of the I and II helices is prevented in the deoxy-G5 hammerhead. Vector I−III (Figure 3B) undergoes a small increase in E_{FRET} in the low magnesium ion concentration range, but remains at a value of around 0.26 under most conditions. This distance therefore remains significantly shorter than that seen in the natural sequence in the presence of 25 mM magnesium ions (where E_{FRET} becomes 0.23). Despite these differences, the behavior of vector III−II (Figure 3C) is quite close to that of the natural sequence, exhibiting a pronounced fall in E_{FRET} in the 0−500 μM magnesium ion concentration range. The FRET efficiencies measured in the presence of 20 mM magnesium ions (summarized in Figure 8) are quite similar to those found for the natural hammerhead sequence in the presence of 500 μM magnesium ions, indicating that the G5-modified hammerhead species has folded into the intermediate stage but is blocked from undergoing further folding.

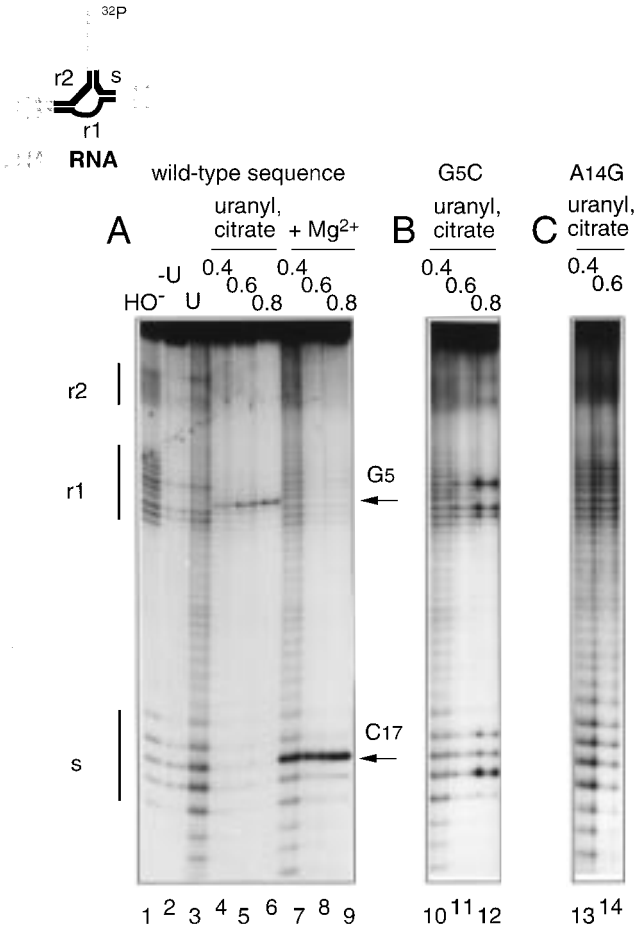

FIGURE 4: Uranyl ion induced photocleavage of the hammerhead ribozyme and 2-folding mutant sequences. The hammerhead ribozyme was constructed in the form of a cloverleaf molecule (insert) where the core (black) comprised RNA and the extremities (grey) were made of DNA (insert, top). Thus there are three sections of RNA in the molecule, called s, r1, and r2 as shown. The molecule was radioactively [5′-^{32}P]-labeled at the 5′ terminus. The wild-type and mutant sequence species were subject to irradiation with light at 420 nm in the presence of 1 mM uranyl nitrate and the concentrations of citrate noted below, with or without magnesium ions. The products of photocleavage were analyzed by separation on a sequencing gel and autoradiography. (A) Wild-type hammerhead ribozyme. Tracks 4−6, uranyl photocleavage in the absence of magnesium ions, with increasing citrate concentration. Note the strong band corresponding to photocleavage at G5 (arrowed, right). Tracks 7−9, uranyl photocleavage in the presence of 5 mM magnesium ions, with increasing citrate concentration. Photocleavage at G5 is suppressed in the presence of magnesium ions, and ribozyme cleavage at C17 is now present (arrowed, right). The positions corresponding to the RNA sections are revealed by base hydrolysis (track 1) and are indicated (left). Track 2, control incubation in the absence of uranyl ions. Track 3, control incubation in the absence of irradiation. Tracks 4 and 7, 0.4 mM citrate; tracks 5 and 8, 0.6 mM citrate; tracks 6 and 9, 0.8 mM citrate. (B) G5C mutant hammerhead. Uranyl photocleavage in the absence of magnesium ions, with increasing citrate concentration. Track 10, 0.4 mM citrate; track 11, 0.6 mM citrate; track 12 0.8 mM citrate. (C) A14G mutant hammerhead. Uranyl photocleavage in the absence of magnesium ions, with increasing citrate concentration. Track 13, 0.4 mM citrate; track 14, 0.6 mM citrate.

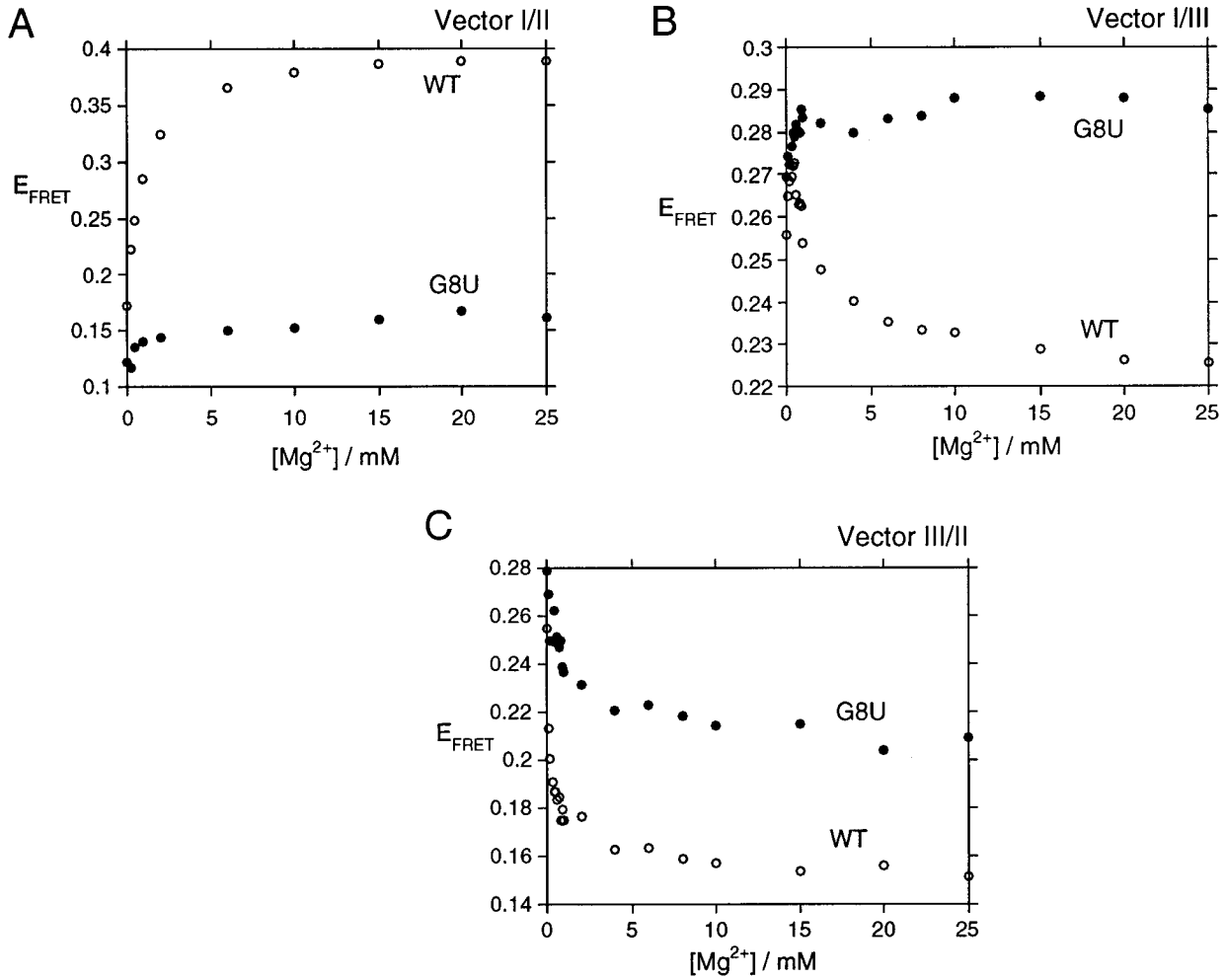

FIGURE 5: Comparison of the ion-induced folding of wild-type and G8U mutant hammerhead ribozymes. All titrations were carried out over the range from 0 to 25 mM magnesium ions. Plot of E_{FRET} as a function of magnesium ion concentration for vector I−II (A), vector I−III (B), and vector III−II (C). Symbols used in all graphs: ○ wild-type hammerhead sequence, ● G8U hammerhead species.

Interactions with Metal Ions in Hammerhead Folding Mutants: Uranyl-Induced Photocleavage Reactions. The FRET analysis shows that the magnesium ion induced folding of the natural hammerhead ribozyme occurs in two stages, each of which appears to be the response to the binding of a single ion (*6*). We have previously shown that uranyl-induced photocleavage can be used to probe metal ion binding in the hammerhead ribozyme (*5*) and revealed the presence of a specific site of uranyl binding close to G5. It is therefore of interest to ask how this interaction is affected by mutations that alter or prevent the folding. For this we chose the mutants A14G to reflect total blockage of folding and G5C to represent folding blocked at the intermediate stage.

In these experiments we used a cloverleaf form of the hammerhead ribozyme, that is formed from a single strand (Figure 4). The core of the ribozyme comprises RNA, while the outer sections are substituted by deoxyribose nucleotides; the molecule therefore contains three sections of RNA, called s, r1, and r2. Unlike the molecules used in the FRET experiments, these contain ribocytidine at position 17 and are therefore potentially active ribozymes. This species was radioactively [5′-^{32}P]-labeled and subjected to irradiation by light of 420 nm wavelength in the presence of 1 mM uranyl nitrate in the presence of increasing concentrations of citrate. The phosphodiester backbone becomes broken because of photocleavage induced by a nearby bound uranyl ion, and thus separation of the radioactive products on a sequencing gel can reveal the position of the bound ion. The results are shown in Figure 4. For the natural sequence, as we have shown previously (*5*), there is a pronounced site of photocleavage at G5 (tracks 4−6), indicating that the ion is bound at or close to this position. The photocleavage is very specific, being largely restricted to a single nucleotide; little cleavage is apparent elsewhere in the r1 segment, nor is cleavage apparent in the s or r2 segments of RNA. When the photoprobing experiments were repeated in the presence of 5 mM magnesium ions (tracks 7−9), the photocleavage at G5 was suppressed and a new band due to ribozyme cleavage at C17 became evident. This indicates a competition between magnesium and uranyl ions for binding to the site near G5.

When we compare this with the photocleavage of the G5C mutant (blocked at the intermediate folding stage), we see that the pattern of backbone breakage is quite different, giving photocleavage on either side of G5 and additional cleavage in the s segment, ie around the position of ribozyme cleavage for the active species. Some cleavage also occurred in the oligopurine sequence in segment r2. Clearly the perturbation of the folding of the G5C mutant results in altered ion-binding properties. When we go further and prevent folding totally with the A14G mutation, the entire

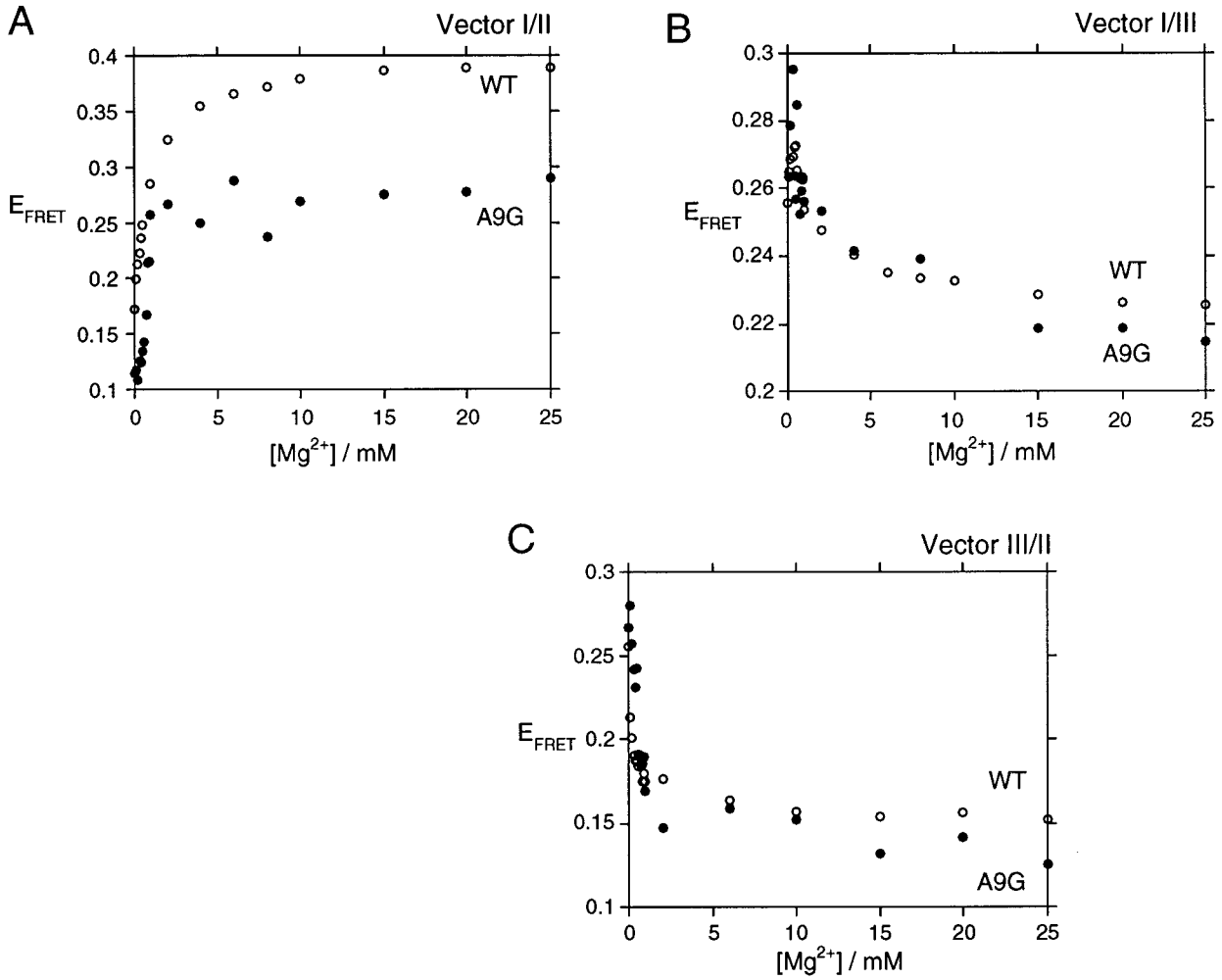

FIGURE 6: Comparison of the ion-induced folding of wild-type and A9G mutant hammerhead ribozymes. All titrations were carried out over the range from 0 to 25 mM magnesium ions. Plot of E_{FRET} as a function of magnesium ion concentration for vector I−II (A), vector I−III (B) and vector III−II (C). Symbols used in all graphs: ○ wild-type hammerhead sequence, ● A9G hammerhead species.

core of the hammerhead becomes subject to photocleavage in a nonspecific way, with extensive photocleavage throughout segments s, r1, and r2. This suggests that the whole of this region is left open to attack by the uranyl ion under these conditions, consistent with an unfolded structure with an open core region. This is consistent with the global structure of the A14G mutant deduced from the FRET studies.

G8U Mutation: Another Severe Folding Block. We examined other mutations in the core of the hammerhead ribozyme that might be expected to influence the ion-dependent folding process. Since domain 2 is formed from an interaction between bases of the oligopurine single-stranded section lying between stems II and III and the 3′ end of the long single-stranded section between stems I and II, we decided to make changes in the latter region. G8U is a mutation that is known to result in complete loss of cleavage activity in the ribozyme (*7*). The fluorescent species based on this mutant sequence were constructed as before, and the FRET analyses of the magnesium ion-induced folding carried out (Figure 5). Vector I−II (Figure 5A) undergoes very little increase in E_{FRET} over the entire range of magnesium ion concentration, showing that the structure remains essentially extended with a long I−II distance. Vector I−III (Figure 5B) exhibits a small increase in E_{FRET}, consistent with some decrease in the I−III distance. Vector III−II (Figure 5C) undergoes a small decrease in E_{FRET} with increased magnesium ion concentration, but the magnitude of this effect is not consistent with the formation of the coaxial stack of helices II and III. Taken together, the results suggest that the G8U mutation leads to a severe block of ion-induced folding, leading to a structure that is largely extended. The structure in the presence of 20 mM magnesium ions is essentially unfolded (the FRET efficiencies are summarized in Figure 8), with a long I−II distance, but with a degree of movement of helix III toward helix I indicating some ion-induced structural rearrangement.

A9G Mutation: A More Subtle Perturbation of Folding. Given the strong effect of the G8U mutation on the folding of the hammerhead ribozyme, it is of interest to examine the effect of changing its neighboring base A9, which also participates in the formation of domain 2. We prepared the fluorescent species corresponding to the mutant ribozyme A9G and performed the FRET analyses of magnesium ion dependent folding (Figure 6). The results indicate that the folding of this mutant sequence is relatively mildly perturbed. The sharp reduction in the E_{FRET} for the vector III−II over the low magnesium ion concentration range (Figure 6C) indicates that helices II and III undergo near-normal coaxial stacking. The final value of E_{FRET} for vector I−III (Figure 6B) is similar in both natural and mutant hammerhead sequences, although the initial shortening is less clear for

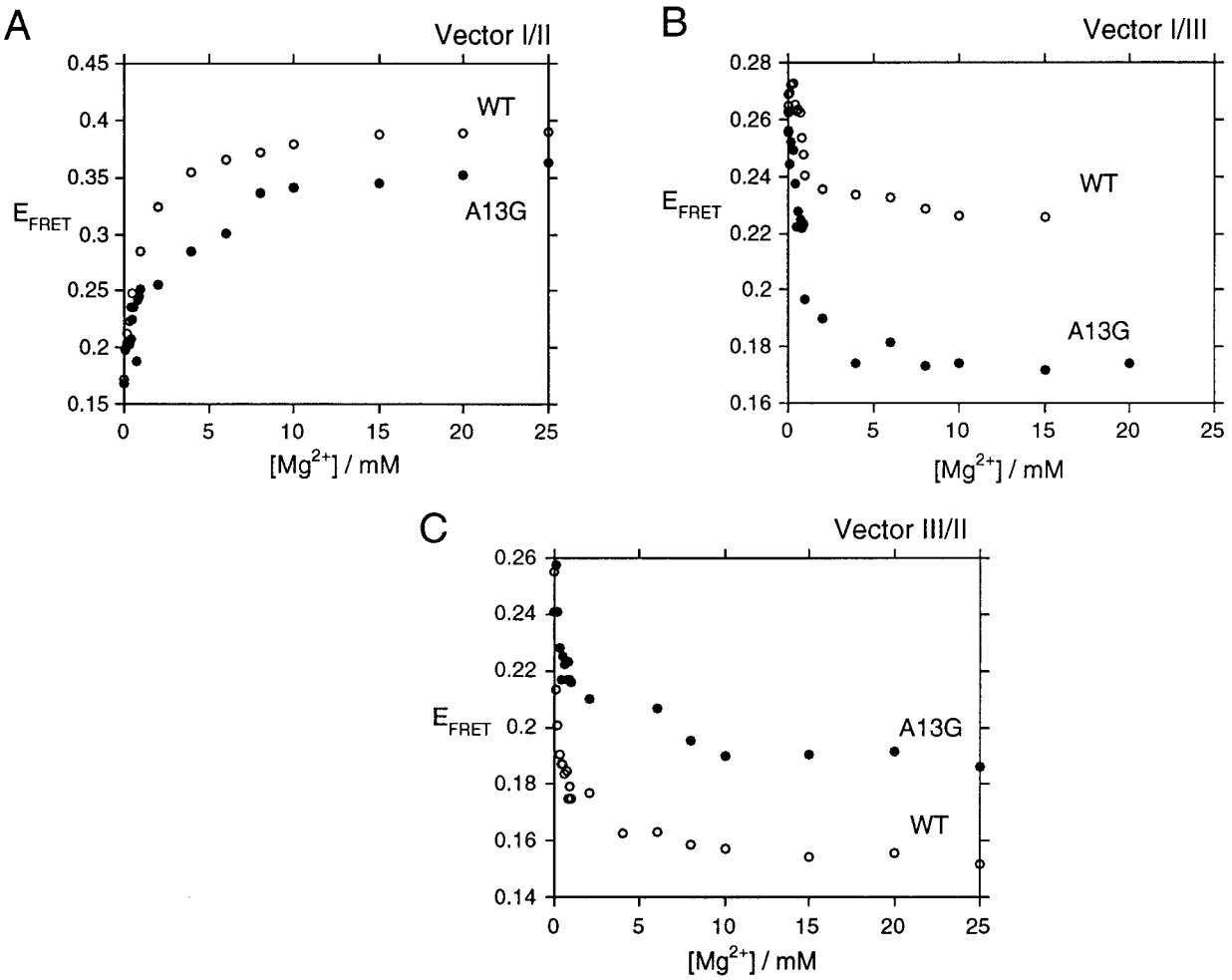

FIGURE 7: Comparison of the ion-induced folding of wild-type and A13G mutant hammerhead ribozymes. All titrations were carried out over the range from 0 to 25 mM magnesium ions. Plot of E_{FRET} as a function of magnesium ion concentration for vector I−II (A), vector I−III (B) and vector III−II (C). Symbols used in all graphs: ○ wild-type hammerhead sequence, ● A13G hammerhead species.

the mutant sequence. Vector I−II (Figure 6A) exhibits the largest deviation between natural and mutant ribozyme, while the A9G mutant undergoes a marked increase in E_{FRET}; the ultimate value achieved at high magnesium ion concentration is significantly lower than that for the natural-sequence molecule (E_{FRET} = 0.29). Thus this mutation has had some effect on the structure adopted in the presence of magnesium ions. However, this structural difference might be relatively subtle, such as a rotation of helix I about its long axis for example. The values of E_{FRET} in the presence of 20 mM magnesium ions (summarized in Figure 8) suggest that this mutation has the smallest effect on the folding of the ribozyme and that the global structure achieved is quite close to that of the natural ribozyme.

A13G Mutation: A Misfolding Mutation. While all the mutations examined so far can be regarded to a first approximation as being blocked at a given stage of the folding process, we have previously found a mutation in the oligopurine sequence between helices II and III (A13U) that leads to misfolding into a new global conformation, deduced from comparative gel electrophoresis (*21*). In this study we have used FRET to examine another mutation at this position, A13G (Figure 7). While the E_{FRET} values for vector I−II (Figure 7A) change with added magnesium ions in a closely similar manner for both natural and A13G sequences, the other two vectors show greater divergence between wild-type and mutant ribozymes. Vector III−II (Figure 7C) exhibits a reduction in E_{FRET} for the A13G sequence in the low magnesium ion concentration range, but this is less pronounced than that for the natural ribozyme, ultimately achieving an efficiency of 0.19. This indicates that the coaxial stacking of helices II and III is perturbed by this mutation. In the same magnesium ion concentration range, the E_{FRET} value for vector I−III (Figure 7B) falls to a level below that observed for any other hammerhead species, with a value of 0.17. This value would be consistent with a coaxial stacking of helices I and III in this mutant RNA. Thus the structure in the presence of 20 mM magnesium ions (summarized in Figure 8) is characterized by long I−III and III−II end-to-end distances and a short I−II distance. This indicates that while the A13G mutation does not prevent magnesium ion dependent folding, it causes a misfolding into a new global structure that is not normally adopted by the natural sequence.

DISCUSSION

We have previously deduced a two-stage folding process for the hammerhead ribozyme (*5*, *6*), induced by the addition of divalent metal ions such as magnesium. In light of the crystal structures (*8*−*10*) we have proposed that the first stage (0−500 μM magnesium ions) involves the formation of domain 2, in which the oligopurine G12A13A14 sequence

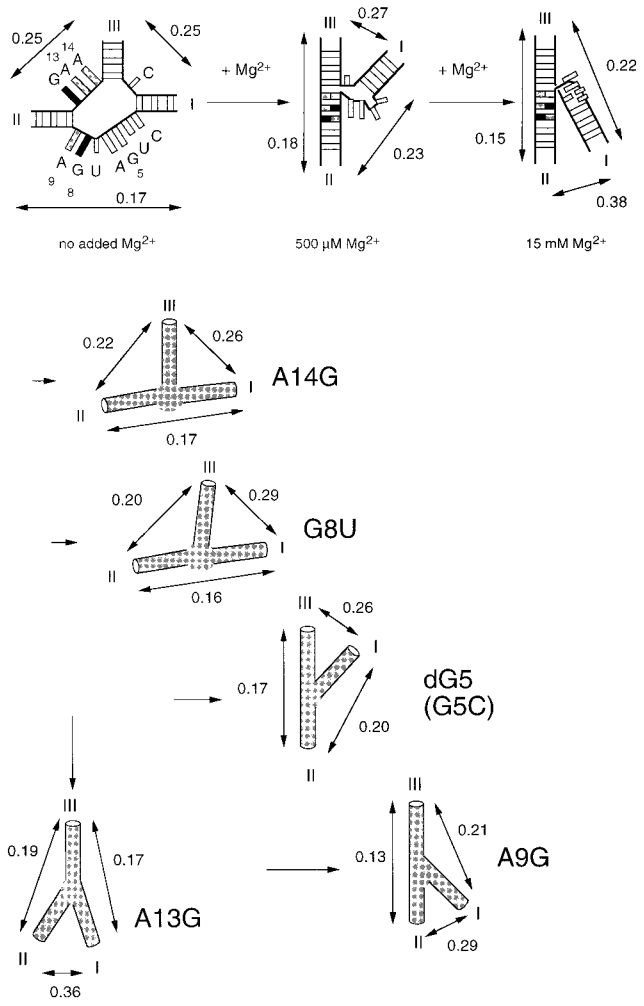

FIGURE 8: Summary of magnesium ion induced folding in the hammerhead ribozyme and mutants. The top shows the proposed two-stage pathway for the ion-induced folding of the hammerhead, with the FRET efficiencies for the three end-to-end vectors at each stage (corresponding to 0, 0.5, and 15 mM magnesium ions). The first stage of the proposed pathway consists of the formation of the domain 2 structure giving the coaxial interaction between stems II and III. In the second stage domain 1 forms by the folding of the C3U4G5A6 sequence and results in a movement of stem I toward stem II. The global structure of the mutant ribozymes in the presence of 20 mM magnesium ions are shown below, with the FRET efficiencies for the end-to-end vectors indicated. The positions correspond approximately to the degree of folding along the normal pathway. Note that the A13G mutant has folding into a different structure, and thus does not lie along this folding pathway.

interacts with the U7G8A9 sequence generating a coaxial interaction between helices II and III. The second stage of the ion-induced folding (1−20 mM magnesium ions) involves principally the C3U4G5A6 sequence, which undergoes a folding into the domain 1 uridine turn structure (Figure 8). Our analyses of hammerhead structures containing point mutations in the core region are consistent with this folding pathway.

Our FRET studies demonstrate that the A14G mutation prevents the folding from occurring at the first stage, ie causing a near-total block to ion-induced folding of the ribozyme. This extends our earlier conclusions from comparative gel electrophoresis (*5*, *21*). Small changes in FRET efficiencies can be observed with increased magnesium ion concentration, but the structure clearly remains essentially unfolded even in the presence of 25 mM magnesium ions. Uranyl ion induced photocleavage of the A14G ribozyme indicates that the entire central core of the molecule is accessible to attack. We have now shown that changing other bases in this region of the ribozyme can also have severe effects on folding. FRET analysis shows that the A13G mutation leads to a misfolded structure, while our earlier comparative gel electrophoresis data indicated that severe misfolding resulted from an A13U mutation (*21*). Mutations on the other strand participating in the formation of domain 2 can also have major effects on folding; the G8U mutation results in a severe block to folding almost equivalent to that of the A14G mutation. The small differences between the FRET efficiencies for the A14G and G8U mutant hammerhead species probably reflect slightly different positions in a folded−unfolded equilibrium, but clearly both species are heavily biased toward the unfolded side. Both mutations in principle allow new Watson−Crick base pairs to be made; perhaps the added rigidity prevents folding in the hammerhead core. Our results point to the importance of the G8•A13 pairing in the formation of the correctly folded structure. The relatively small (although not negligible) structural effect of the A9G mutation is perhaps surprising, suggesting that a G•G pairing can be tolerated at this position without disrupting the global conformation to a large degree.

The second stage of the ion-induced folding is blocked by changes at G5, and our FRET analysis shows that removal of the 2′ hydroxyl group at G5 prevents the formation of domain 1, while not interfering with the formation of domain 2 to a first approximation. This confirms our earlier analysis by comparative gel electrophoresis, where we also showed that the G5C mutation causes a similar block to folding at the stage corresponding to the formation of domain 1. These results indicate that G5 does not participate in the formation of domain 2, as would be expected, but that it plays an important role in the transition into the folded structure of domain 1. The pattern of uranyl ion induced photocleavage of the G5C hammerhead structure is different from that of the wild-type sequence, yet is consistent with a structure that is less accessible than the A14G mutant. This indicates a state of partial folding, consistent with the FRET and comparative gel electrophoresis results, and shows that the discrete uranyl binding site close to G5 is formed late in the folding process. Ion interaction close to this position has also been indicated by the effect of Sp phosphorothioate substitution at A6 on ribozyme cleavage (*22*) and by the discovery of a binding site for a terbium ion (*23*). From the crystal structures of the hammerhead ribozyme it might be expected that the structure would be tolerant of sequence changes at G5, since the base is not involved in intramolecular interactions. Thus the effect of the G5C mutation is perhaps surprising; however, this mutation also has a major effect on the activity of the ribozyme (*7*), so there is a correlation between the structural and functional observations based on changes at this position.

While our results support the two-stage ion-induced folding process outlined before, they also show that folding of the hammerhead ribozyme is probably more complicated than this. Although the assembly of domain 2 largely occurs in the first transition, there is some relaxation of this structure shown by the continued if more gentle, reduction in FRET efficiency for vector III−II during the second transition, and

it is interesting that this readjustment at higher magnesium ion concentration is not observed in the deoxy G5 hammerhead structure, which is blocked in the second transition. The two transitions should probably not therefore be regarded as being completely independent, and long-range effects of metal ion binding on the cleavage reaction have been proposed (*24*).

It is interesting that a single change in sequence can also direct the ion-induced folding into a new global structure, as shown by the mutations at A13. This indicates that the folding can be directed into a different pathway, and may suggest that even the natural sequence could become trapped in misfolded structures. The common observation of incomplete cleavage by ribozyme preparations has been attributed to subfractions of incorrectly folded material that may be kinetically trapped in that conformation (*25*). It is important to note that all the mutant sequences that we have studied exhibit perturbed folding of one kind or another. This underlines the facility with which the ion-induced folding is perturbed by small changes of sequence, and this is consistent with the observations that most of the core sequence of the hammerhead ribozyme cannot be altered without loss of catalytic activity to one degree or another (*7*). It also serves as a warning that changes in activity of mutated ribozymes cannot necessarily be interpreted in terms of the removal or replacement of selected functional groups, because any given mutation might have resulted in a more general alteration in the structure of the ribozyme.

MATERIALS AND METHODS

Chemical Synthesis of RNA-Containing Oligonucleotides. Oligonucleotides containing both DNA and RNA sections were synthesized using phosphoramidite chemistry implemented on a Applied Biosystems 394 DNA/RNA synthesizer. RNA was synthesized using ribonucleotide phosphoramidites with 2′-butyldimethylsilyl protection. Fluorescein (PE-ABI) and indocarbocyanine (Cy3, Glen Research) were coupled to the 5′ termini as phosphoramidites. Oligoribonucleotides were deprotected and purified as described previously (*6*).

Construction of Hammerhead Species for FRET Analysis. The hammerhead constructs used in this study comprised the core and three arms, each of 10 bp in length. The terminal base pair of each arm were constructed from deoxynucleotides, as this allowed for a more efficient coupling of the fluorescent dye on the 5′ end of the molecule. The basic hammerhead species was constructed from three oligonucleotides:

strand S:

5′ C**GUAGUACGUCUGAGCGGUC**G 3′

strand R1:

5′ C**GACCGCUCACUGAUGAGGCCCACTC**G 3′

strand R2:

5′ C**GAGUGGGCCGAAACGUACUAC**G 3′

Underlined bases indicate deoxyribose substitution. All versions of strand S contained deoxyribose substitution at C17 to prevent self-cleavage occurring in the presence of magnesium ions. In addition to these unlabeled oligonucleotides, each was synthesized with 5′ fluorescein or Cy3 fluorophores.

Hammerhead species for FRET studies were assembled from one unlabeled strand, one strand labeled with fluorescein, and one Cy3-labeled strand, thus placing the required fluorescein−Cy3 pair at the ends of chosen arms. The fluorescent species were constructed and purified as described previously (*6*).

Fluorescence Spectroscopy. Fluorescence spectra were recorded at 5 °C using an SLM-Aminco 8100 fluorimeter operating in photon counting mode, and spectra were corrected for lamp fluctuations and instrumental variations, as described in (ref *6*). Polarization artifacts were avoided by setting excitation and emission polarizers at 54.74°. Values of E_{FRET} were measured using the $(ratio)_A$ method (*14, 18*). An extracted acceptor spectrum $F^A(\nu_1, \nu')$ (excitation at $\nu' = 490$ nm, with emission at ν_1) is normalized to a second spectrum ($F(\nu_2, \nu'')$) from the same sample excited at a wavelength ($\nu'' = 547$ nm) at which only the acceptor is excited, with emission at ν_2. We then obtain the acceptor ratio:

$$(\text{ratio})_A = F^A(\nu_1, \nu')/F(\nu_2, \nu'') = \{E_{FRET}\, d^+ (\epsilon^D(\nu')/\epsilon^A(\nu'')) + (\epsilon^A(\nu')/\epsilon^A(\nu''))\}(\Phi^A(\nu_1)/\Phi^A(\nu_2)) \quad (1)$$

Superscripts D and A refer to donor and acceptor, respectively. ϵ^D and ϵ^A are the molar absorption coefficients at the indicated frequency of donor and acceptor, respectively, and Φ^A is the fluorescent quantum yield of the acceptor. E_{FRET} may be calculated from $(ratio)_A$ since $\epsilon^D(\nu')/\epsilon^A(\nu'')$ and $\epsilon^A(\nu')/\epsilon^A(\nu'')$ are measured from absorption spectra, and $\Phi^A(\nu_1)/\Phi^A(\nu_2)$ is unity when $\nu_1 = \nu_2$.

Fluorescence anisotropy (r) was determined from measurements of fluorescence intensities using vertical excitation and emission polarizers ($F_{||}$), and vertical excitation and horizontal emission polarizers ($F_\perp$, corrected for polarization artifacts). Fluorescence anisotropy was calculated from:

$$r = (F_{||} - F_\perp)/(F_{||} + 2F_\perp) \quad (2)$$

Uranyl Photocleavage. Cloverleaf hammerhead ribozyme molecules with an RNA core were prepared by chemical synthesis and assembled as described previously (*5*), with wild-type, A14G, or G5C sequences. Uranyl photocleavage experiments were performed using 200 cps of the radioactive hammerhead RNA in 100 μL volumes in 50 mM Tris·HCl (pH 7.2) containing 1 mM uranyl nitrate and the magnesium and citrate concentrations indicated in the text. Samples were irradiated for 20 min by exposure to a fluorescent tube (Phillips TI 40 W/03) emitting light at 420 nm. Following irradiation, sodium acetate (pH 4.5) was added to a final concentration of 0.3 M and the RNA was precipitated by ethanol. The pellet was redissolved in 88% formamide containing xylene cyanol and bromophenol blue, and the cleavage products were analyzed by denaturing gel electrophoresis in 15% polyacrylamide gels in 90 mM Tris·borate (pH 8.3), 2.5 mM EDTA containing 7 M urea. The radioactive bands were visualized by autoradiography. An RNA sequence ladder was obtained by heating the radioac-

tive hammerhead construct for 1 min at 90 °C in the presence of 0.2 M NaOH.

ACKNOWLEDGMENT

We thank Frank Walter and Bob Clegg for discussion and the Cancer Research Campaign and the Biotechnology and Biological Sciences Research Council for financial support.

REFERENCES

1. Hutchins, C. J., Rathjen, P. D., Forster, A. C., and Symons, R. H. (1986) *Nucleic Acids Res. 14*, 3627−3640.
2. Forster, A. C., and Symons, R. H. (1987) *Cell 49*, 211−220.
3. Hazeloff, J. P., and Gerlach, W. L. (1988) *Nature 334*, 585−591.
4. Uhlenbeck, U. C. (1987) *Nature 328*, 596−600.
5. Bassi, G., Møllegaard, N. E., Murchie, A. I. H., von Kitzing, E., and Lilley, D. M. J. (1995) *Nat. Struct. Biol. 2*, 45−55.
6. Bassi, G. S., Murchie, A. I. H., Walter, F., Clegg, R. M., and Lilley, D. M. J. (1997) *EMBO J. 16*, 7481−7489.
7. Ruffner, D. E., Stormo, G. D., and Uhlenbeck, O. C. (1990) *Biochemistry 29*, 10695−10702.
8. Pley, H. W., Flaherty, K. M., and McKay, D. B. (1994) *Nature 372*, 68−74.
9. Scott, W. G., Finch, J. T., and Klug, A. (1995) *Cell 81*, 991−1002.
10. Scott, W. G., Murray, J. B., Arnold, J. R. P., Stoddard, B. L., and Klug, A. (1996) *Science 274*, 2065−2069.
11. Murray, J. B., Terwey, D. P., Maloney, L., Karpeisky, A., Usman, N., Beigelman, L., and Scott, W. G. (1998) *Cell 92*, 665−673.
12. Gast, F. U., Amiri, K. M. A., and Hagerman, P. J. (1994) *Biochemistry 33*, 1788−1796.
13. Menger, M., Tuschl, T., Eckstein, F., and Porschke, D. (1996) *Biochemistry 35*, 14710−14716.
14. Murchie, A. I. H., Clegg, R. M., von Kitzing, E., Duckett, D. R., Diekmann, S., and Lilley, D. M. J. (1989) *Nature 341*, 763−766.
15. Clegg, R. M., Murchie, A. I. H., Zechel, A., Carlberg, C., Diekmann, S., and Lilley, D. M. J. (1992) *Biochemistry 31*, 4846−4856.
16. Clegg, R. M., Murchie, A. I. H., Zechel, A., and Lilley, D. M. J. (1993) *Proc. Natl. Acad. Sci. U.S.A. 90*, 2994−2998.
17. Murchie, A. I. H., Thomson, J. B., Walter, F., and Lilley, D. M. J. (1998) *Molecular Cell 1*, 873−881.
18. Clegg, R. M. (1992) *Methods Enzymol. 211*, 353−388.
19. Tuschl, T., Gohlke, C., Jovin, T. M., Westhof, E., and Eckstein, F. (1994) *Science 266*, 785−789.
20. Amiri, K. M. A., and Hagerman, P. J. (1994) *Biochemistry 33*, 13172−13177.
21. Bassi, G. S., Murchie, A. I. H., and Lilley, D. M. J. (1996) *RNA 2*, 756−768.
22. Knoll, R., Bald, R., and Fürste, J. P. (1997) *RNA 3*, 132−140.
23. Feig, A. L., Scott, W. G., and Uhlenbeck, O. C. (1998) *Science 279*, 81−84.
24. Peracchi, A., Beigelman, L., Scott, E. C., Uhlenbeck, O. C., and Herschlag, D. (1997) *J. Biol. Chem. 272*, 26822−26826.
25. Uhlenbeck, O. C. (1995) *RNA 1*, 4−6.

BI982985R